Supplementary information

Cyclic cataluminescence method enabled by heterogeneous electron allocator for multiple aldehydes detection in tea

Huiting Chen[#], Mengmeng Ji[#], Ling Xia, Yufei Hu*, Gongke Li*

School of Chemistry, Sun Yat-sen University, Guangzhou 510006, China

*Corresponding authors:

cesgkl@mail.sysu.edu.cn (Gongke Li)

huyufei@mail.sysu.edu.cn (Yufei Hu)

# Huiting Chen and Mengmeng Ji contributed equally.

Materials and chemical reagents

Acetaldehyde, 2-methylbutyral, pentanal, n-heptanaldehyde, ethanol, acetophenone, acetic acid, benzaldehyde, linalool, geranyl, cyclohexanol, methyl benzoate, ethyl benzoate, 2-heptanone, nitric acid, gadolinium nitrate hexahydrate, urea and MgO were purchased from Aladdin Reagent Co., LTD. (Shanghai, China). All reagents were analytically pure and used directly without further purification. Carbon nanotubes were prepared by Time Nano (outer diameter greater than 50 nm, length: 0.5-2 μm, purity greater than 98%). Deionized water was used in all experiments.

Instruments

The Biological & Physical Chemiluminescence (BPCL) weak chemiluminescence instrument was acquired from the Institute of Biophysics, Chinese Academy of Sciences (Beijing, China). The voltage controller was obtained from Xiechang Voltage Equipment Manufacturing Co., Ltd., Shanghai, China. The peristaltic pump (FAT200.8) was sourced from Xinweicheng Technology Co., Ltd. (Chengdu, China). The electromagnetic valve was procured from Valco Instrument Co., Ltd. (The United States). The ceramic heater core was purchased from Huiyou Electronics Co., Ltd. (Zhuhai, China). Gas chromatography-mass spectrometry (GC-MS) was purchased from Agilent Technologies. The morphology, and constituents of the catalysts were analyzed using scanning electron microscopy (SEM), D8 ADVANCE X-ray powder diffractometer (XRD, Bruker, Germany) characterized the crystal structure of the materials, X-ray photoelectron spectroscopy (XPS, K-Alpha+), thermogravimetric analyzer (TG 209 F3 Tarsus), and surface area and porosity analyzer (Micromeritics ASAP 2020M), respectively.

Gas chromatography-mass spectrometry program

The concentrations of acetaldehyde, pentanal and 2-methylbutyral in tea were determined by GC-MS. Column: DB-WAXeter quartz capillary column (60 m × 0.25 mm, inner diameter 0.25 μm, film thickness 0.25 μm). Carrier gas was nitrogen. Inlet temperature was 280°C, heating conditions was at the initial temperature of 130°C, keep for 1 min and rise to 280°C at 10 °C/min for 3 min. Ion source temperature was 230°C. Quadrupole temperature was 150°C. Column flow rate was 1.00 mL/min.

Construction and operation of CCTL system

The cyclic cataluminescence (CCTL) system included a self-made reaction chamber, a voltage controller, a BPCL ultra-weak luminescence analyzer with a photomultiplier tube as the detector, a peristaltic pump, a three-way valve, and a miniature electric six-way solenoid valve. The reaction chamber was a self-made quartz tube, in which a ceramic heating rod coated with solid catalyst was placed. Polytetrafluoroethylene (PTFE) hoses were used to connect pump and valve components. The three-way valve was directly connected to port of the six-way solenoid valve, and the two inlet ports of the reaction chamber were connected to ports of the microelectric six-way solenoid valve, forming a circuit. By changing the working state of the solenoid valve, the direction of the current carrying capacity could be automatically changed within a specified period. Therefore, when the sample was injected into the CCTL system, chemicals of different cycles can repeatedly pass through the reaction pool, resulting in a series of chemiluminescence signals that conform to the exponential decay equation.

CCTL measurement procedure

After stabilization of the instrument, the analytical sample is injected into the three-way valve through the gas injection needle. After mixing the air, analytical sample flows through the quartz tube and is oxidized by oxygen in the air on the catalyst surface. During the test, the circuit is changed by altering the working state of the solenoid valve, so that the reaction substances of different periods flow through the reaction pool and produce a series of chemiluminescence signals. The luminescence signal is directly measured by BPCL ultra-weak chemiluminescence analyzer.

Computational details

All calculations were performed using the first-principles tool, Vienna Ab initio Simulation Package (VASP). All density functional theory (DFT) calculations were performed in the generalized gradient approximation (GGA) using the Perdew-Burke-Ernzerhof (PBE) formula. The projected augmented wave (PAW) potential was used to describe the ion core and a plane-wave basis set was used to account for valence electrons with a kinetic energy cutoff of 450 eV. The Kohn-Sham orbital was partially occupied with a width of 0.05 eV. Brillouin zone integration was performed using 1 × 1 × 1 gamma center sampling. The adsorption energy E_{ads} was calculated using the following equation:

$$E_{ads}=E_{total}-E_{surface}-E_{gas} \qquad \text{(Formula S1)}$$

where E_{total} represents the total energy of the gas molecules on the catalyst surface system, $E_{surface}$ and E_{gas} represent the energies of the catalyst surface and isolated molecules, respectively. The smaller E_{ads} is, the easier the gas adsorbed.

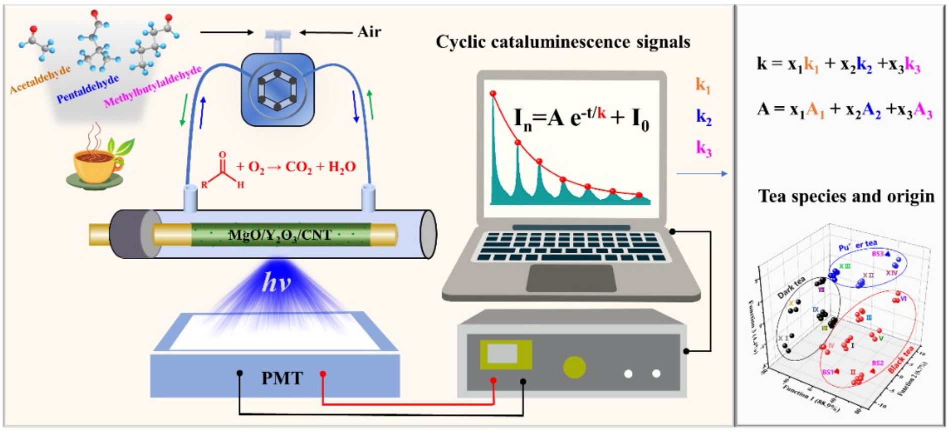

Fig. S1 Schematic of the cyclic cataluminescence system.

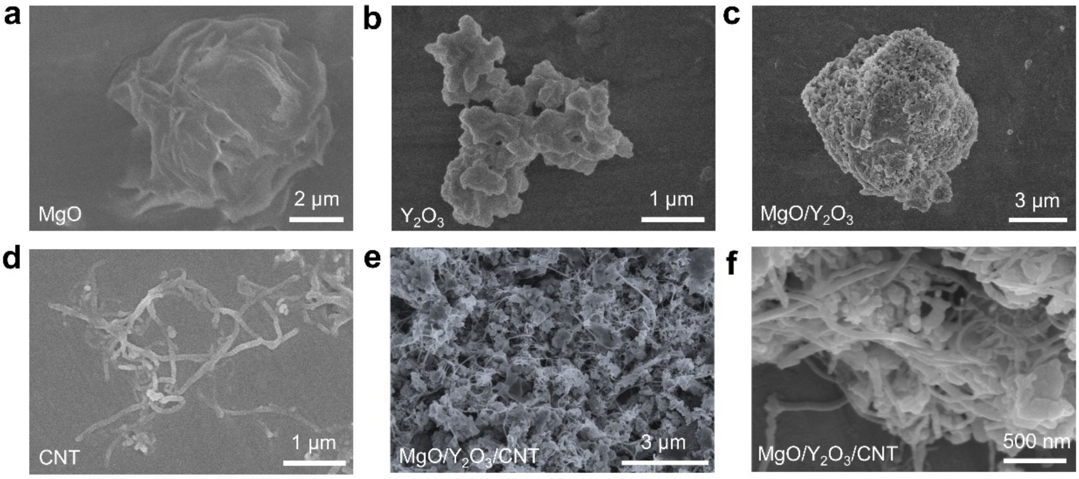

Fig. S2 SEM characterization (a) MgO, (b) Y_2O_3, (c) MgO/Y_2O_3, (d) CNT, and (e) $MgO/Y_2O_3/CNT$.

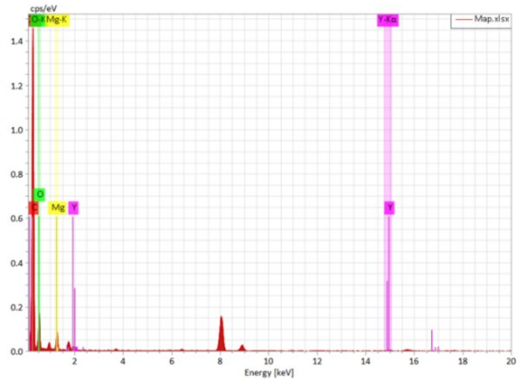

Fig. S3 EDS of $MgO/Y_2O_3/CNT$ catalyst.

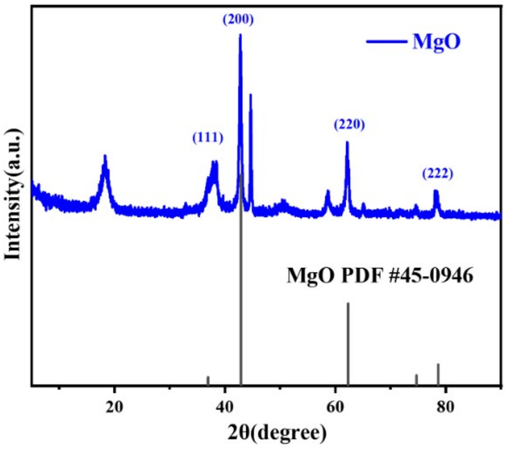

Fig. S4 XRD pattern of MgO.

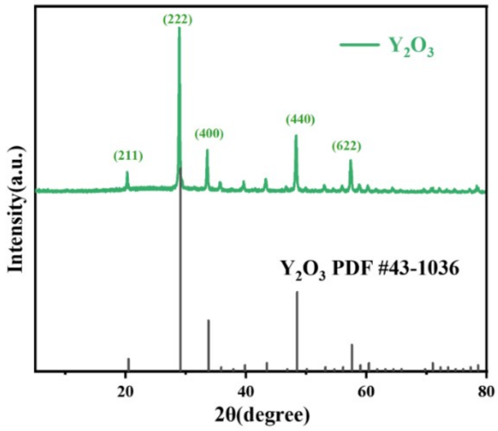

Fig. S5 XRD pattern of Y_2O_3.

Table S1 Estimation of crystallite size of MgO and Y_2O_3 using XRD data.

Parameter	MgO	Y_2O_3
2θ (deg)	42.9	29.1
FWHM (deg)	0.3	0.4
D(nm)	26	21

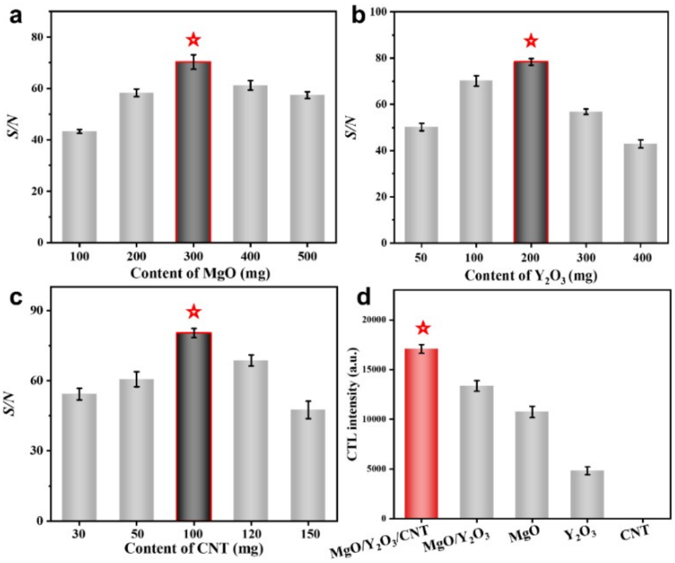

Fig. S6 Optimization of MgO/Y_2O_3/CNT catalyst (a) MgO addition (b) Y_2O_3 addition (c) CNT addition. (d) CCTL intensity of acetaldehyde on different catalysts. (Concentration: 8.0 mg/L; rotational speed: 35 rpm; detection wavelength: 440 nm; temperature: 210°C)

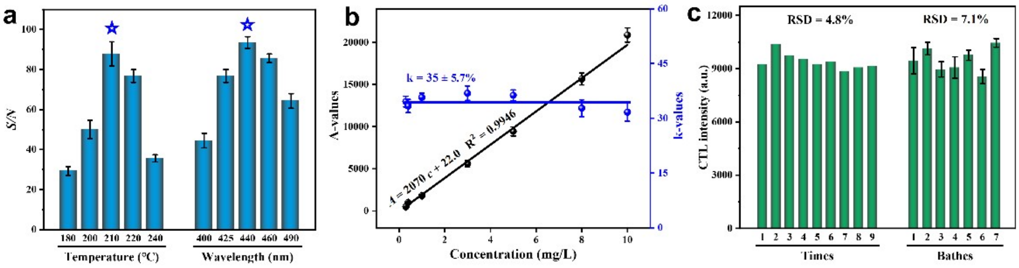

Fig. S7 Study on influencing factors of CCTL (a) temperature, detection wavelength and (b) acetaldehyde concentration. (c) CTL intensity of acetaldehyde applied for 9 consecutive times on $MgO/Y_2O_3/CNT$ surface and CTL intensity of acetaldehyde on the surface of 7 batches $MgO/Y_2O_3/CNT$. (Concentration: 5.0 mg/L; rotational speed: 35 rpm; detection wavelength: 440 nm; temperature: 210°C)

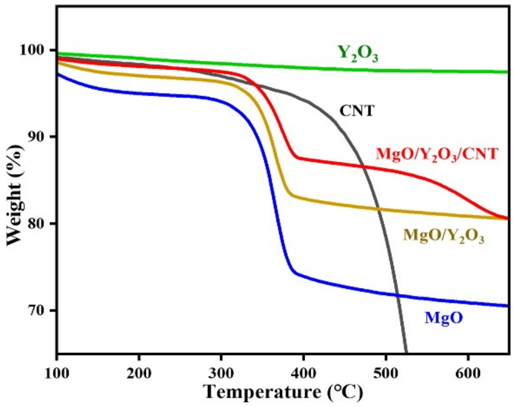

Fig. S8 Catalysts characterization of thermogravimetric curve.

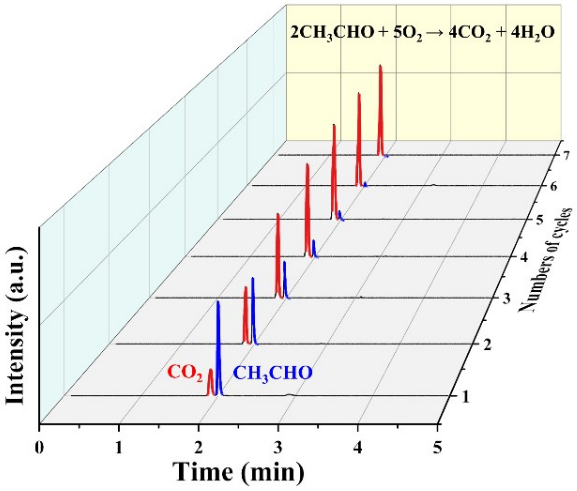

Fig. S9 GC-MS chromatogram of catalytic oxidation of acetaldehyde.

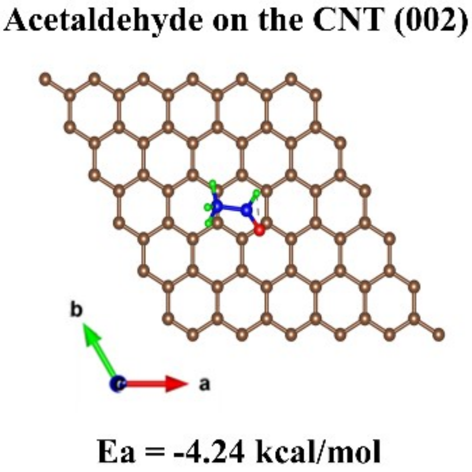

Fig. S10 Adsorption capacity of CNT (002) for acetaldehyde.

Table S2. The measured and theoretical values of binary components A and k^a

pentanal (w, %)	acetaldehyde (w, %)	A_m	A_t	Relative error (%)	k_m	k_t	Relative error (%)
0	100	18025	18025	0	38.1	38.1	0
20	80	17402	16324	6.6	30.5	34.0	-10.3
50	50	15357	13773	11.5	25.4	27.8	-8.6
80	20	9426	11221	-16.0	23.6	21.5	9.8
100	0	9521	9521	0	17.4	17.4	0

(a. k_m and A_m: measured values, k_t and A_t: theoretical values)

Table S3. The measured and theoretical values of ternary components *A* and *k*

pentanal (*w*, %)	acetaldehyde (*w*, %)	2-methylbutyraldehyde (*w*, %)	A_m	A_t	Relative error (%)	k_m	k_t	Relative error (%)
33	33	33	12510	11017	13.6	20.8	19.7	5.6
25	25	50	8375	9807	-14.6	17.3	15.9	8.8
0	0	100	5840	5840	0	4.1	4.1	0
25	50	25	14100	12853	9.7	22.7	24.4	-7.0
0	100	0	18025	18025	0	38.1	38.1	0
50	25	25	8862	10727	-17.4	21.5	19.3	11.4
100	0	0	9521	9521	0	17.4	17.4	0

Table S4. Comparison of the CCTL method with other methods for identifying tea origin.

Method	Sample pretreatment	Equipment cost	Detection time	Sensitivity	Accuracy	Ref.
GC-MS	Complexity	Expensive	20-30 min	μg/L	90%	[1]
NIRS	Simple	Expensive	5 min	-	99%	[2]
HSI	Simple	Expensive	5 min	-	100%	[3]
E-nose	Simple	Inexpensive	2-5 min	μg/L	100%	[4]
CCTL	Simple	Inexpensive	2-5 min	mg/L	100%	This work

[1] S. Luo, Y. Shen, W. Cheng, N. Wang, Y. Zhang, J. Wang, D. Chang, J. Li, X. Guo, H. Gao, Food Chem. 2026, 512, 148901

[2] H. Xia, W. Chen, D. Hu, A. Miao, X. Qiao, G. Qiu, J. Liang, W. Guo, C. Ma, Food Chem. 2024, 440, 138242.

[3] X. Ge, J. Sun, B. Lu, Q. Chen, W. Xun, Y. Jin, J. Food Process Eng. 2019, 42, e13289.

[4] F. Li, X. Wang, S. Zhou, D. Wang, Z. Gong, M. Fan, ACS Food Sci. Technol. 2022, 2, 1096-1102.